Human M2 Macrophages Limit NK Cell Effector Functions through Secretion of TGF-β and Engagement of CD85j

Sol Y. Nuñez,* Andrea Ziblat,* Florencia Secchiari,* Nicolás I. Torres,* Jessica M. Sierra,* Ximena L. Raffo Iraolagoitia,*,[1] Romina E. Araya,*,[2] Carolina I. Domaica,* Mercedes B. Fuertes,* and Norberto W. Zwirner*,[†]

NK cells play important roles during immunosurveillance against tumors and viruses as they trigger cytotoxicity against susceptible cells and secrete proinflammatory cytokines such as IFN-γ. In addition, upon activation, macrophages can become proinflammatory (M1) or anti-inflammatory (M2) cells. Although the consequences of the cross-talk between M1 and NK cells are known, the outcome of the cross-talk between M2 and NK cells remains ill-defined. Therefore, in the current work, we investigated the outcome and the underlying mechanisms of the interaction between resting or stimulated human NK cells with M1 or M2. We observed a lower percentage of activated NK cells that produced less IFN-γ upon coculture with M2. Also, $CD56^{dim}$ NK cells cocultured with M2 displayed lower degranulation and cytotoxic activity than NK cells cocultured with M1. Soluble TGF-β and M2-driven upregulation of CD85j (ILT-2) on NK cells accounted for the diminished IFN-γ production by $CD56^{bright}$ NK cells, whereas M2-driven upregulation of CD85j on NK cells accounted for the generation of hyporesponsive $CD56^{dim}$ NK cells with limited degranulation and cytotoxic capacity. Accordingly, M2 expressed higher amounts of HLA-G, the main ligand for CD85j, than M1. Hyporesponsiveness to degranulation in NK cells was not restored at least for several hours upon removal of M2. Therefore, alternatively activated macrophages restrain NK cell activation and effector functions through different mechanisms, leading to NK cells that display diminished IFN-γ production and at least a transiently impaired degranulation ability. These results unravel an inhibitory circuit of possible relevance in pathological situations. ***The Journal of Immunology*****, 2018, 200: 1008–1015.**

Natural killer cells play a crucial role during immunosurveillance against tumors, viruses, and other intracellular pathogens, inducing cytotoxicity of susceptible target cells and secreting cytokines such as IFN-γ (1, 2). Also, they are abundant in different tissues, including secondary lymphoid organs where they exert immunoregulatory functions and shift the adaptive immune response toward a Th1 and $CD8^+$ cytotoxic-mediated immunity (3). Two major subpopulations of NK cells have been identified in peripheral blood of humans: ∼90% are $CD3^-CD56^{dim}CD16^+$ cells and display a strong cytotoxic activity, whereas the rest are $CD3^-CD56^{bright}CD16^{dim/-}$, produce immunoregulatory cytokines, and are poorly cytotoxic (4, 5). Activation of NK cells is determined by the balance of signals triggered upon engagement of a vast array of activating or inhibitory cell surface receptors (2, 6).

Macrophages are key players during inflammation and tissue homeostasis that can differentiate into a broad range of fully functional cells that vary between proinflammatory (M1) and anti-inflammatory (M2) macrophages (7, 8). M1 macrophages are characterized by high expression of MHC class II molecules, CD86, CD274 (PD-L1), and others, secretion of proinflammatory cytokines (such as IL-1, IL-6, TNF, IL-12, IL-23, and IL-18), and production of NO (7, 9, 10). Conversely, M2 macrophages display lower expression of these cell surface markers but express higher amounts of mannose receptor (CD206) and scavenger receptors (MARCO and CD163), and secrete low amounts of proinflammatory cytokines (7, 9, 10). Polarization of human macrophages into different effector subsets has been associated with many immunopathological conditions and diseases (11).

The interaction between NK cells and M1 has been explored (12–14) but the consequences of their interaction with M2 remain ill-defined (15). M2 resemble tumor-associated macrophages (TAMs) (11), whose expansion and recruitment have been associated with poor prognosis in different tumor types because of local and systemic effects that facilitate tumor growth, angiogenesis, metastases, and immunosuppression (16–19). As NK cell phenotype and effector functions are compromised in cancer (20, 21), it is possible that TAMs and their closely related M2 induce immunosuppressive

*Laboratorio de Fisiopatología de la Inmunidad Innata, Instituto de Biología y Medicina Experimental, C1428ADN Buenos Aires, Argentina; and [†]Departamento de Química Biológica, Facultad de Ciencias Exactas y Naturales, Universidad de Buenos Aires, C1428EGA Buenos Aires, Argentina

[1]Current address: Cancer Research UK Beatson Institute, Bearsden, Glasgow, U.K.

[2]Current address: Center for Cancer Research, National Cancer Institute, National Institutes of Health, Bethesda, MD.

ORCIDs: 0000-0002-7856-2973 (S.Y.N.); 0000-0001-6872-0598 (F.S.); 0000-0002-8891-4821 (X.L.R.I.); 0000-0001-9787-2670 (R.E.A.); 0000-0002-2734-1468 (M.B.F.).

Received for publication May 23, 2017. Accepted for publication November 28, 2017.

This work was supported by grants from the Agencia Nacional de Promoción Científica y Tecnológica, the Consejo Nacional de Investigaciones Científicas y Técnicas de Argentina, and the University of Buenos Aires (all to N.W.Z.), and by donations from Fundación Williams and Fundación René Barón to Instituto de Biología y Medicina Experimental. S.Y.N., A.Z., N.I.T., F.S., and J.M.S. are fellows of Consejo Nacional de Investigaciones Científicas y Técnicas de Argentina and C.I.D., M.B.F., and N.W.Z. are members of its Researcher Career.

Address correspondence and reprint requests to Dr. Norberto W. Zwirner, Laboratorio de Fisiopatología de la Inmunidad Innata, Instituto de Biología y Medicina Experimental, Vuelta de Obligado 2490, C1428ADN Buenos Aires, Argentina. E-mail address: nzwirner@ibyme.conicet.gov.ar

The online version of this article contains supplemental material.

Abbreviations used in this article: CM, conditioned media; FC, flow cytometry; IC, isotype control; MFI, median fluorescence intensity; pfp, perforin; rMFI, relative MFI; TAM, tumor-associated macrophage.

effects in NK cells that might impact on their immunosurveillance capacity. Accordingly, the aim of this study was to explore the consequences of the interaction between human M2 and NK cells, and to unravel the underlying mechanisms that might contribute to their suppression.

Materials and Methods

Reagents

Human IL-12 and IL-15 (PeproTech), IL-18 (MBL International), IFN-γ and M-CSF (ImmunoTools), IL-4 (R&D Systems), TGF-β1 (Tonbo), LPS (*Escherichia coli* 0111:B4 strain; Sigma-Aldrich), Zombie Green (BioLegend), and 4,5-Diaminofluorescein diacetate (DAF-2 DA; Calbiochem) were used. The following mAbs were used for flow cytometry (FC): FITC anti-CD14 (M5E2), PE/Cy7 anti-CD274 (29E.2A3), PE anti-CD86 (IT2.2), APC-Cy7 anti-CD206 (15-2), APC anti-CD56 (N901; Beckman Coulter), PE/Cy7 anti-CD3 (UCHT1; Tonbo), FITC anti-CD69 (FN50), PE anti-CD25 (BC96), PE or BV421 anti–IFN-γ (4S.B3), FITC anti-CD107a (H4A3), FITC anti–T-bet (4B10), PE anti-NKG2D (1D11), PE anti-NKp30 (P30-15), PE anti-NKp46 (9E2), PE anti-NKp80 (5D12), Alexa Fluor 488 anti-perforin (anti-pfp; dG9), PE anti-CD178 (FasL, NOK-1) (all from BioLegend), Alexa Fluor 488 anti-NKG2C (134591), FITC anti-CD85j (292305), PE anti-NKG2A (131411), PE anti-TIGIT (741182), Alexa Fluor 488 anti-TRAIL (71908) (all from R&D Systems), FITC anti–DNAM-1 (DX11), FITC anti-KIR3DL1 (DX9) (both from BD Biosciences), PE anti-granzyme B (GB11; eBioscience), and PE anti–HLA-G (MEMG9; Abcam). The following mAbs were used for blocking/neutralization experiments: anti–TGF-β (1D11.16.8), anti-CD85j (GHI/75), mouse IgG1κ isotype control (IC) (MOPC-21), all from BioLegend, and mouse IgG2bκ IC (eBMG2b) from eBioscience. Normal human gammaglobulin (IgG_{2500}) was from Purissimus (Argentina).

Cells and cultures

Monocytes and NK cells were isolated from blood from healthy volunteers (provided by the Blood Bank of the Province of Buenos Aires or by the Hospital Churruca-Visca of Buenos Aires). Studies have been approved by the institutional review committee and informed consent of participating subjects was obtained. Monocytes ($CD14^+$ cells) were isolated by MACS (Miltenyi Biotec) and NK cells were isolated using RosetteSep (Stemcell). Purity of isolated cells was always above 90%, as assessed by FC ($CD14^+$ or $CD3^-CD56^+$ cells). Cells were cultured in RPMI 1640 (Life Technologies) supplemented with 10% inactivated FBS (Life Technologies) and sodium pyruvate (Fluka). To obtain unpolarized macrophages (M0), monocytes were cultured for 6 d with 100 ng/ml M-CSF. To obtain M1 and M2, M0 were cultured for 24 h with 100 ng/ml LPS and 50 ng/ml IFN-γ or 200 ng/ml IL-4, respectively. M1 and M2 were cocultured with freshly isolated NK cells (1:1 ratio) in the absence or in the presence of 10 ng/ml IL-12, 1 ng/ml IL-15, and 10 ng/ml IL-18 for 18 h. For autologous cultures, NK cells were frozen when monocytes were isolated and thawed before coculture experiments. To obtain conditioned media (CM), M1 or M2 were washed and cultured for 24 h with fresh medium. NK cells cocultured with M1 or M2 (1:1 ratio) in the absence or in the presence of IL-12, IL-15, and IL-18 were harvested and used for phenotypic and functional characterization by FC. IFN-γ and/or degranulation were also assessed in NK cells stimulated with IL-12, IL-15, and IL-18 or K562 cells (from American Type Culture Collection) separated from macrophages using 24-well 0.4-μm pore size transwell devices (1:1 ratio), in NK cells stimulated with the cytokines in the presence of CM from M1 or M2 and an IC mAb, or an anti–TGF-β neutralizing mAb, or in NK cells stimulated with the cytokines and increasing concentrations of recombinant TGF-β for 24 h. For degranulation, K562 cells and a FITC-labeled anti-CD107a mAb were added during the last 5 h of culture, and CD107a expression in NK cells was assessed as described (22). K562 is the universal target cell line for NK cell–mediated cytotoxicity derived from a chronic myelogenous leukemia. In some experiments, NK cells were cocultured with M1 or M2 in the presence of an IC mAb or an anti-CD85j blocking mAb. In additional experiments, after coculture with M1 or M2 for 24 h, NK cells were separated from macrophages by immunomagnetic depletion of $CD14^+$ cells and further cultured alone or with fresh M1 or M2, in the presence of an IC mAb or an anti-CD85j neutralizing mAb for 5 h. These NK cells were used to assess degranulation.

Flow cytometry

FC was performed as described (23). Macrophages were harvested with TrypLE Express (Life Technologies). Expression of IFN-γ, T-bet, pfp, and granzyme B was analyzed by intracellular FC using Fix/Perm Buffer (BioLegend). For IFN-γ and CD107a, cells were cultured in the presence of monensin and brefeldin A (BioLegend) solutions for 5 h. Viability was assessed with Zombie Green (BioLegend). To assess NO production, macrophages were harvested and labeled with 4.4 μM DAF-2 DA for 30 min at 37°C, washed and acquired. Cells were analyzed in a FACSCanto II flow cytometer (BD Biosciences) or MACSQuant Analyzer 10 (Miltenyi Biotec). Data were analyzed using FlowJo X software (Tree Star) and results were expressed as median fluorescence intensity (MFI), as relative MFI (rMFI) (MFI of the specific mAb divided by the MFI of the IC mAb), or as percentage of positive cells.

ELISA for cytokines

IFN-γ secretion was analyzed by ELISA as described (23). Secretion of IL-12 and IL-10 was assessed using the ELISA MAX Standard kit (BioLegend). Secretion of IL-23, IL-27, and TGF-β was assessed using the human IL-23, IL-27, and TGF-β1 DuoSet (R&D Systems). Secretion of IL-18 was assessed using the anti-human IL-18 matched pair of mAb clone 125-2H and biotinylated clone 159-12B (R&D Systems) and HRP-labeled streptavidin (BioLegend).

NK cell–mediated cytotoxicity

NK cells were cultured with M1 or M2 for 18 h. Thereafter, eFluor Dye 670 (eBioscience) –labeled K562 was added at different E:T ratios (1:1, 3:1, 5:1). After 5 h, cells were harvested, labeled with Zombie Green, and analyzed by FC. Percentage of cytotoxicity was calculated as 100 × percentage of eFluor Dye 670^+Zombie $Green^{high}$ cells / percentage of eFluor Dye 670^+ cells.

Conjugates

eFluor Dye 670–labeled NK cells were cultured with M1 or M2 for 18 h and mixed with CFSE-labeled K562 cells at an E:T ratio of 1:1. Then, NK cell–target cell conjugates were evaluated as described (23).

Statistical analysis

A one-way ANOVA with Bonferroni post hoc test was used to compare three or more experimental groups, a paired *t* test was used to compare two experimental groups, and a two-way ANOVA with repeated measures matched by both factors and Bonferroni post hoc test was used for functional and blocking experiments. Data were analyzed using GraphPad Prism 6.0 software.

Results

M2 macrophages restrain NK cell activation

To interrogate the consequences of the interaction between M2 and NK cells, we obtained unpolarized human macrophages (M0), M1, and M2, as outlined in Fig. 1A. Phenotypic and functional analysis revealed that as expected, M1 displayed increased expression of CD86 and CD274, whereas M2 displayed increased expression of CD206 (Fig. 1B, 1C). Also, M1 produced more NO (Fig. 1D, 1E) and secreted higher amounts of IL-12, IL-23, IL-27, IL-18, and IL-10 and similar amounts of TGF-β compared with M2 (Fig. 1F). Nonetheless, the ratio of secretion of IL-12 to IL-10 and IL-12 to TGF-β was significantly higher for M1 than for M2 (Fig. 1G). A similar effect was observed for the ratio of IL-18, IL-23, or IL-27 to IL-10 or TGF-β (data not shown).

Next, we explored their effect on NK cell activation (Fig. 2). We observed that only M1 but not M2 induced a statistically significant increase in the percentage of $CD56^{dim}$ cells expressing CD69. In addition, stimulation of NK cells with IL-12, IL-15, and IL-18 induced high percentages of $CD56^{bright}$ and $CD56^{dim}$ NK cells expressing CD25 (Fig. 2A, 2B) and CD69 (Fig. 2C, 2D), but these percentages were lower in the presence of M2 than in the presence of M1. Also, $CD56^{dim}$ NK cells exposed to M2 displayed lower expression of CD56 than those exposed to M1 (Fig. 2E, 2F), confirming that M2 preclude full NK cell activation. Of note, M1 and M2 did not affect the viability of NK cells (data not shown).

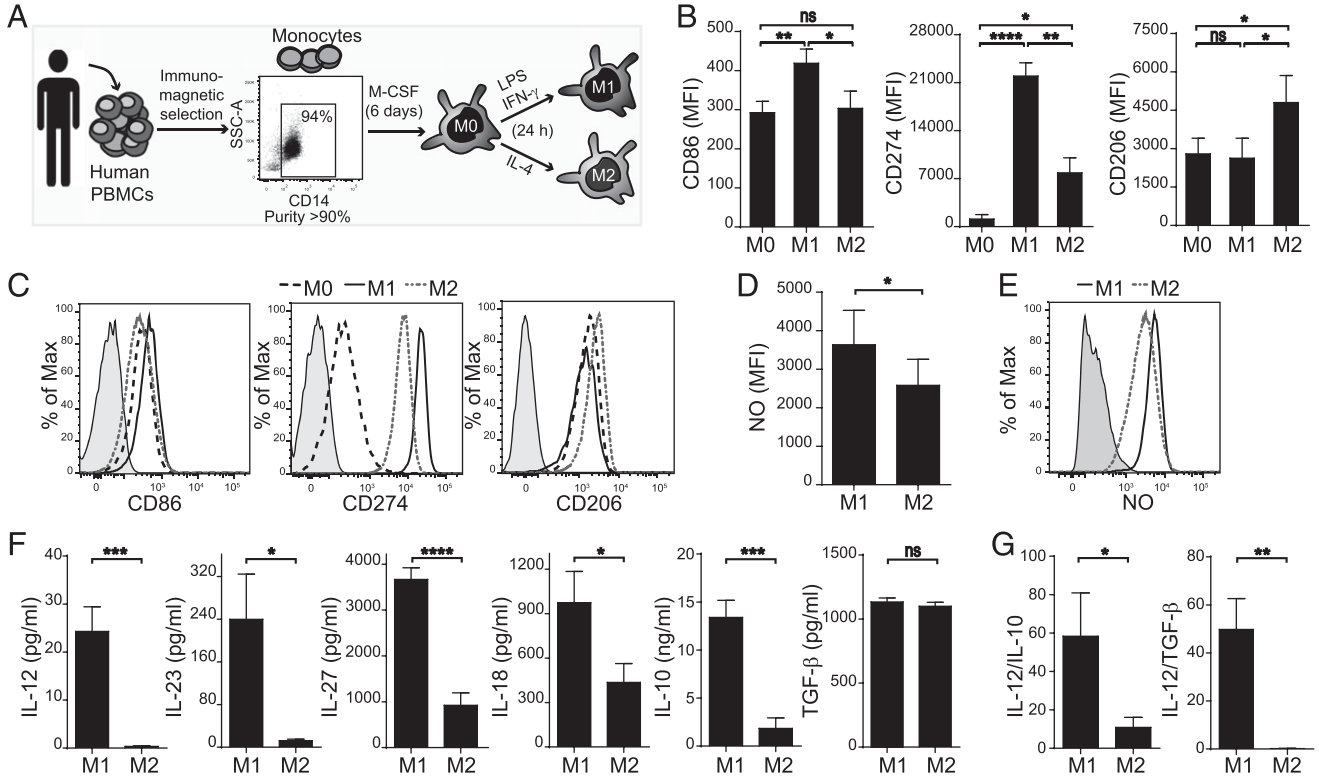

FIGURE 1. In vitro differentiated M1 and M2 display a different phenotype and secretion pattern of cytokines. (**A**) Protocol used to obtain unpolarized and polarized human macrophages. CD14$^+$ cells isolated from blood from healthy donors were differentiated to M0 with M-CSF for 6 d and exposed overnight to LPS and IFN-γ or IL-4 to obtain M1 and M2 macrophages, respectively. (**B**) Phenotypic characterization of M0, M1, and M2 by FC ($n = 9$). (**C**) Representative histograms from macrophages from one healthy donor. (**D**) Production of NO by M1 and M2 by FC ($n = 7$). (**E**) Representative histograms from macrophages from one healthy donor. (**F**) Production of IL-12, IL-23, IL-27, IL-18, IL-10, and TGF-β by M1 and M2 ($n = 16$, $n = 13$, $n = 9$, $n = 7$, $n = 19$, $n = 15$, respectively). (**G**) Ratio of secretion of IL-12 to IL-10 ($n = 14$) and IL-12 to TGF-β ($n = 14$). A one-way ANOVA with Bonferroni post hoc test was used in (B). A paired t test was used in (D), (F), and (G). Mean ± SEM were plotted in (B), (D), (F), and (G). $^*p < 0.05$, $^{**}p < 0.01$, $^{***}p < 0.001$, $^{****}p < 0.0001$.

M2 restrict NK cell IFN-γ production through TGF-β secretion

Next, we assessed the effect of M2 on NK cell effector functions. We observed significantly fewer IFN-γ$^+$ CD56^{bright} NK cells in response to stimulation with IL-12, IL-15, and IL-18 in the presence of M2 than in the presence of M1 or M0 (Fig. 3A, 3B, Supplemental Fig. 1A). A similar effect was observed on CD56^{dim} NK cells but, as expected, the percentage of IFN-γ–producing NK cells was much lower than in CD56^{bright} NK cells (Fig. 3C, 3D). These results were validated using autologous combinations of NK cells and macrophages (Fig. 3E, 3F). Thus, subsequent experiments were performed with allogeneic combinations of macrophages and NK cells. Also, the effect of M2 on IFN-γ secretion was confirmed by ELISA using resting (Fig. 3G) and cytokine-stimulated NK cells (Fig. 3H).

As T-bet is a critical transcription factor that regulates IFN-γ production in T and NK cells, we assessed whether M2 affect T-bet expression in CD56^{bright} NK cells (Fig. 3I, 3J). Indeed, compared with M1, M2 negatively affected T-bet expression in cytokine-stimulated CD56^{bright} NK cells, suggesting that such reduction could be one of the effects of M2 on NK cells that lead to a reduced IFN-γ production. To further explore the underlying mechanisms, we repeated the experiments described in Fig. 3A but using transwell devices (Fig. 4A). Physical separation of NK cells from macrophages did not reverse the inhibitory effect, whereas CM from M2 retained the inhibitory effect on IFN-γ production (Fig. 4B). Thus, M2-derived soluble factors curb IFN-γ production by CD56^{bright} NK cells in response to cytokine stimulation. To identify such factors, we performed neutralization experiments and assessed IFN-γ production. Neutralization of TGF-β but not IL-10 in CM from M2 resulted in an increased percentage of IFN-γ–producing CD56^{bright} NK cells (Fig. 4C–E, Supplemental Fig. 2). Moreover, neutralization of TGF-β in CM from M1 also led to a higher percentage of IFN-γ–producing CD56^{bright} NK cells compared with the IC mAb, suggesting that TGF-β also exerts a negative regulation of IFN-γ production by NK cells exposed to classical proinflammatory macrophages (Fig. 4C, 4D). However, neutralization of TGF-β in CM from M2 led to a significantly higher recovery in the percentage of IFN-γ–producing CD56^{bright} NK cells compared with neutralization of TGF-β in CM from M1 (Fig. 4E). Moreover, stimulation of NK cells with cytokines in the presence of increasing concentrations of TGF-β led to dose-dependent reduction in the percentage of IFN-γ–producing CD56^{bright} NK cells (Fig. 4F) confirming the suppressive effect of TGF-β on IFN-γ production by NK cells. Therefore, TGF-β secreted by M2 strongly contributes to restrain IFN-γ production by CD56^{bright} NK cells.

M2 preclude NK cell–mediated cytotoxicity through engagement of CD85j (ILT-2)

Next, we explored whether M2 also affect the cytotoxic potential of CD56^{dim} NK cells. To this end, NK cells were cocultured with M1 or M2 for 18 h, K562 cells were added, and after 5 h degranulation was assessed in CD56^{dim} NK cells (Fig. 5A, 5B). We observed that M2 significantly inhibited NK cell degranulation compared with M1 and M0 in allogeneic (Fig. 5A, 5B, Supplemental Fig. 1B) and autologous combinations (Fig. 5C). Also, NK cells exposed to M2 were less cytotoxic than NK cells exposed to M1 at

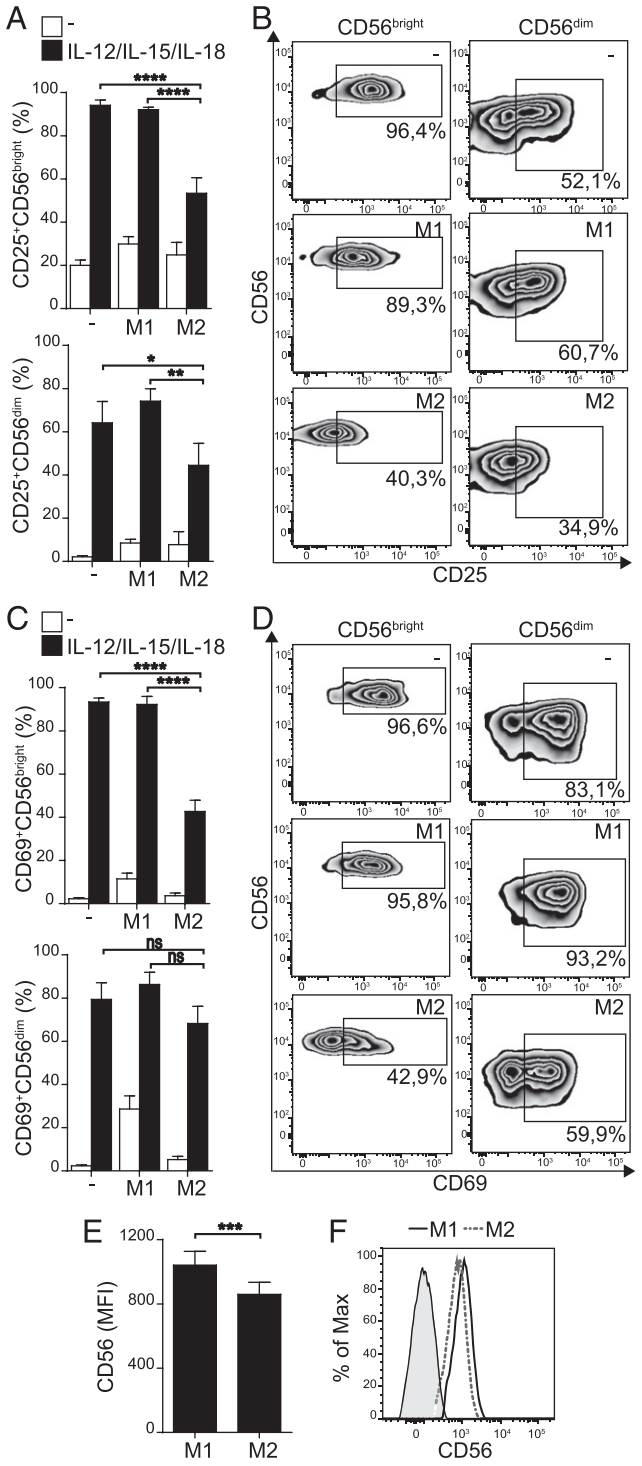

FIGURE 2. M2 negatively affect upregulation of CD25, CD69, and CD56 on NK cells upon stimulation with cytokines. Percentage of CD56^{bright} or CD56^{dim} NK cells expressing CD25 (**A** and **B**) or CD69 (**C** and **D**) after culture in the absence (−) or in the presence of M1 or M2, in the absence (white bars) or in the presence of IL-12, IL-15, and IL-18 (black bars). Representative zebra plots from cells from one healthy donor of results shown in black bars are shown in (B) and (D). A two-way ANOVA with repeated measures matched by both factors and Bonferroni post hoc test was used in (A) and (C) (n = 6). (**E**) MFI of CD56 in CD56^{dim} NK cells after coculture with M1 or M2. A paired t test was used (n = 9). (**F**) Representative histograms from cells from one healthy donor. Mean ± SEM were plotted in (A), (C), and (E). *$p < 0.05$, **$p < 0.01$, ***$p < 0.001$, ****$p < 0.0001$.

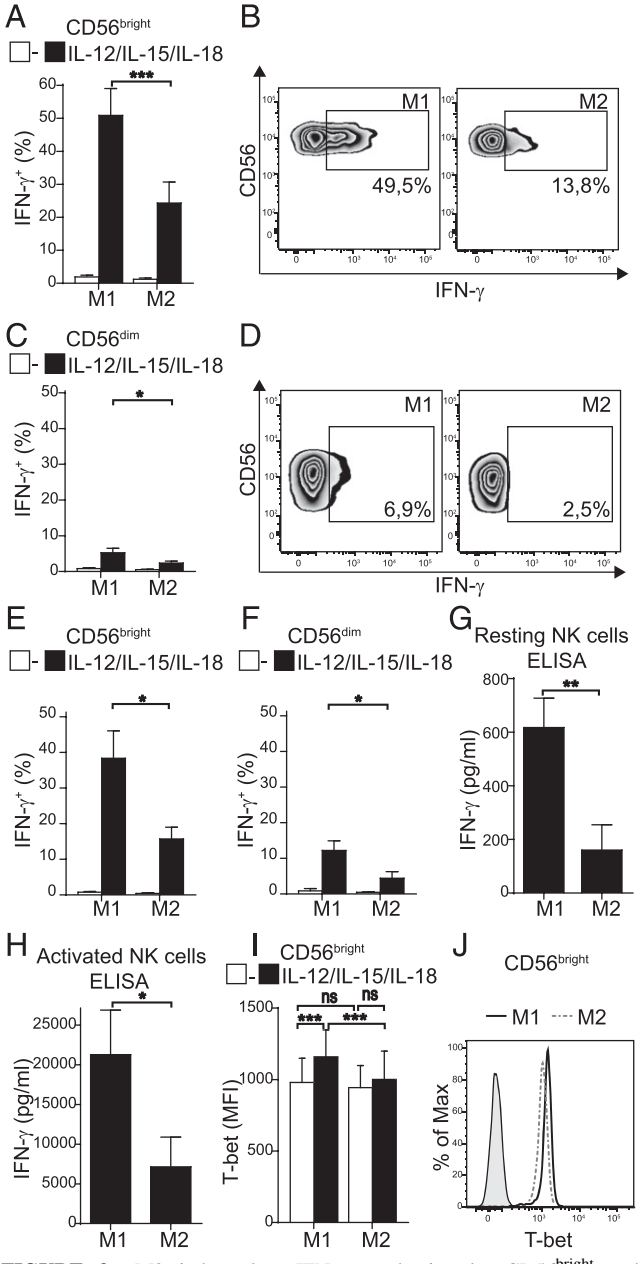

FIGURE 3. M2 induce less IFN-γ production by CD56^{bright} and CD56^{dim} NK cells than M1 upon stimulation with cytokines. Percentage of CD56^{bright} (**A** and **B**) or CD56^{dim} (**C** and **D**) NK cells producing IFN-γ after coculture with allogeneic M0, M1, or M2 in the absence (white bars) or in the presence of IL-12, IL-15, and IL-18 (black bars). Representative zebra plots from cells from one healthy donor are shown in (B) and (D) (n = 6). Percentage of CD56^{bright} (**E**) or CD56^{dim} (**F**) NK cells producing IFN-γ after coculture with autologous M1 or M2 in the absence (white bars) or in the presence of IL-12, IL-15, and IL-18 (black bars) (n = 4). (**G**) Production of IFN-γ by resting NK cells after coculture with allogeneic M1 or M2, assessed by ELISA. (**H**) Production of IFN-γ by NK cells stimulated with IL-12, IL-15, and IL-18 after coculture with allogeneic M1 or M2, assessed by ELISA (n = 8). (**I**) T-bet expression in CD56^{bright} NK cells after coculture with allogeneic M1 or M2 in the absence (white bars) or in the presence of IL-12, IL-15, and IL-18 (black bars) (n = 8). (**J**) Representative histograms from cells from one healthy donor. A two-way ANOVA with repeated measures matched by both factors and Bonferroni post hoc test was used for (A), (C), (E), (F), and (I). A paired t test was used in (G) and (H). Mean ± SEM were plotted in (A), (C), and (E)–(I). *$p < 0.05$, **$p < 0.01$, ***$p < 0.001$.

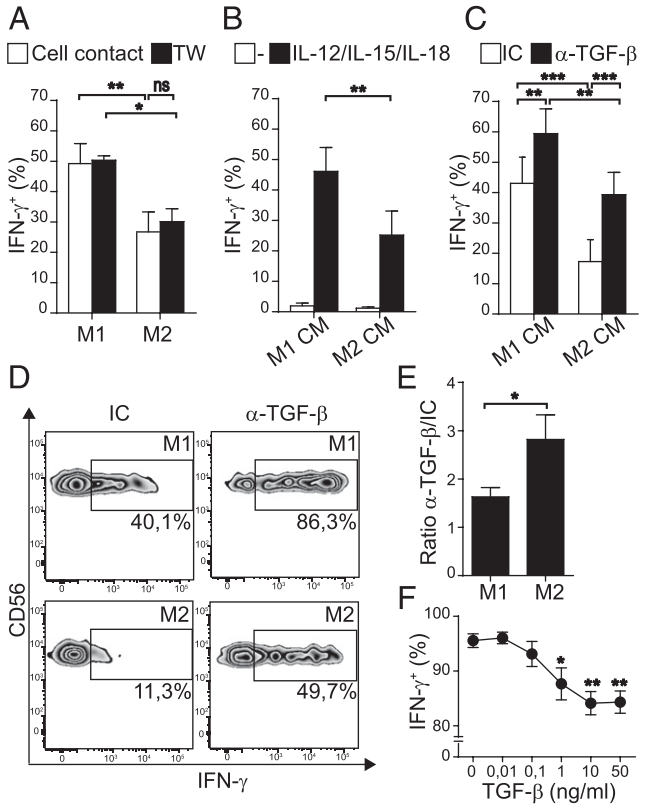

FIGURE 4. Reduced IFN-γ production by CD56^{bright} NK cells induced by M2 upon stimulation with cytokines is due to soluble TGF-β. (**A**) Percentage of IFN-γ–producing CD56^{bright} NK cells stimulated with IL-12, IL-15, and IL-18 after coculture with allogeneic M1 or M2 in the presence of cell-to-cell contact (white bars) or when cells were separated by transwell devices (TW, black bars) (n = 6). (**B**) Percentage of IFN-γ–producing CD56^{bright} NK cells cultured in the presence of CM from M1 or M2 in the absence (white bars) or in the presence of IL-12, IL-15, and IL-18 (black bars) (n = 8). (**C**) Percentage of IFN-γ–producing CD56^{bright} NK cells cultured in the presence of IL-12, IL-15, IL-18, and CM from M1 or M2 in the presence of an IC mAb (white bars) or an anti–TGF-β neutralizing mAb (black bars) (n = 7). (**D**) Representative zebra plots from cells from one healthy donor. (**E**) Ratio of the percentage of IFN-γ–producing CD56^{bright} NK cells in the presence of an anti–TGF-β neutralizing mAb and the percentage of IFN-γ–producing CD56^{bright} NK cells in the presence of an IC mAb for NK cells cultured with CM from M1 or M2 (n = 6). (**F**) Percentage of IFN-γ–producing CD56^{bright} NK cells cultured in the presence of IL-12, IL-15, IL-18 and increasing concentrations of TGF-β (n = 6). A two-way ANOVA with repeated measures matched by both factors and Bonferroni post hoc test was used in (A)–(C). A paired t test was used in (E). A one-way ANOVA and Bonferroni post hoc test was used in (F). Mean ± SEM were plotted in (A)–(C), (E), and (F). *$p < 0.05$, **$p < 0.01$, ***$p < 0.001$.

different E:T ratios (Fig. 5D), confirming that M2 negatively regulate the cytotoxic activity of CD56^{dim} NK cells. Accordingly, compared with M1, M2 negatively affected the content of pfp (Supplemental Fig. 3A) and granzyme B (Supplemental Fig. 3B) in CD56^{dim} NK cells but did not affect the formation of NK cell–target cell conjugates nor the expression of TRAIL and CD178 (data not shown).

To further explore the underlying mechanisms involved in CD56^{dim} NK cell suppression, we assessed NK cell degranulation in response to K562 cells separating NK cells from macrophages using transwell devices. Physical separation of both cells completely prevented the inhibitory effect of M2 on CD56^{dim} NK cell degranulation (Fig. 6A), and CM from M2 did not affect NK cell degranulation (data not shown). Thus, M2 preclude NK cell–mediated cytotoxicity through a cell-to-cell contact-dependent mechanism. Blocking experiments performed with an anti–TGF-β mAb during the coculture ruled out the involvement of membrane-bound TGF-β (data not shown). Thus, we hypothesized that the reduced cytotoxic ability might be associated with the downregulation of activating receptors and/or the upregulation of inhibitory receptors. A phenotypic characterization of NK cells cultured with M1 or M2 revealed no downregulation of the activating receptors CD226 (DNAM-1), CD335 (NKp46), CD337 (NKp30), CD314 (NKG2D), NKp80 (KLRF1), and NKG2C (Supplemental Fig. 3C) or upregulation of the inhibitory receptors NKG2A, TIGIT and KIR3DL1 (Supplemental Fig. 3D). However, we observed that a higher percentage of NK cells expressed CD85j and the expression of this inhibitory receptor was increased in NK cells upon coculture with M2 compared with M1 (Fig. 6B, 6C), whereas M2 expressed significantly higher amounts of its main ligand (HLA-G) than M1 (Fig. 6D, 6E). Therefore, we next explored whether such higher expression of CD85j and HLA-G contributed to the suppressive effect of M2 on the degranulation of CD56^{dim} NK cells. Indeed, blockade of CD85j during coculture with M2 resulted in a partial restoration of the percentage of degranulating CD56^{dim} NK cells (Fig. 6F–H). Strikingly, blockade of CD85j during coculture with M2 led to a significantly higher recovery in the percentage of degranulated CD56^{dim} NK cells compared with blockade during coculture with M1 (Fig. 6G). Of note, the recovery in NK cell degranulation was not detected when this receptor was blocked exclusively on M1 or M2 (Supplemental Fig. 4A), suggesting that the inhibitory effect of CD85j occurs upon engagement of this receptor on NK cells and not on macrophages. Moreover, the blocking effect of this mAb was equally evident when the functional experiments were performed in the presence of an excess of human IgG, which would prevent the hypothetical binding of the

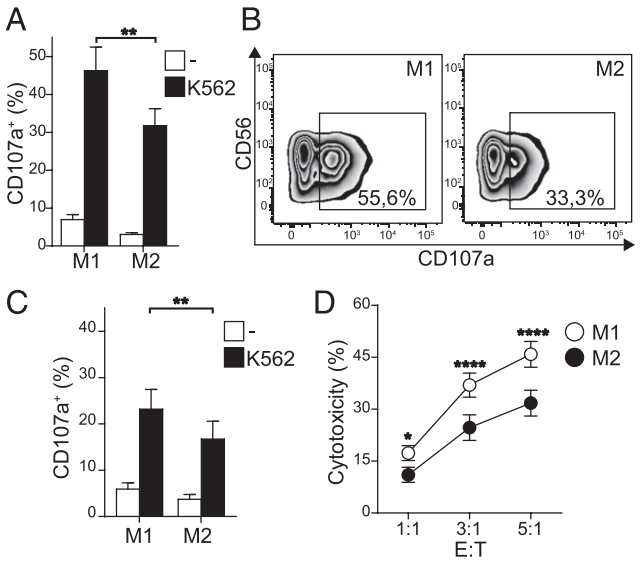

FIGURE 5. M2 induce reduced degranulation and cytotoxic activity of CD56^{dim} NK cells against susceptible target cells than M1. (**A**) Percentage of CD107a^{+}CD56^{dim} NK cells after coculture with allogeneic M1 or M2 in the absence (white bars) or in the presence of K562 target cells (black bars) (n = 8). (**B**) Representative zebra plots from cells from one healthy donor. (**C**) Percentage of CD107a^{+}CD56^{dim} NK cells after coculture with autologous M1 or M2 in the absence (white bars) or in the presence of K562 target cells (black bars) (n = 6). E:T ratio (A–C), 1:1. (**D**) Cytotoxicity of NK cells cocultured with M1 (white dots) or M2 (black dots) against K562 cells at different E:T ratios (n = 6). A two-way ANOVA with repeated measures matched by both factors and Bonferroni post hoc test was used in (A), (C), and (D). Mean ± SEM were plotted in (A), (C), and (D). *$p < 0.05$, **$p < 0.01$, ****$p < 0.0001$.

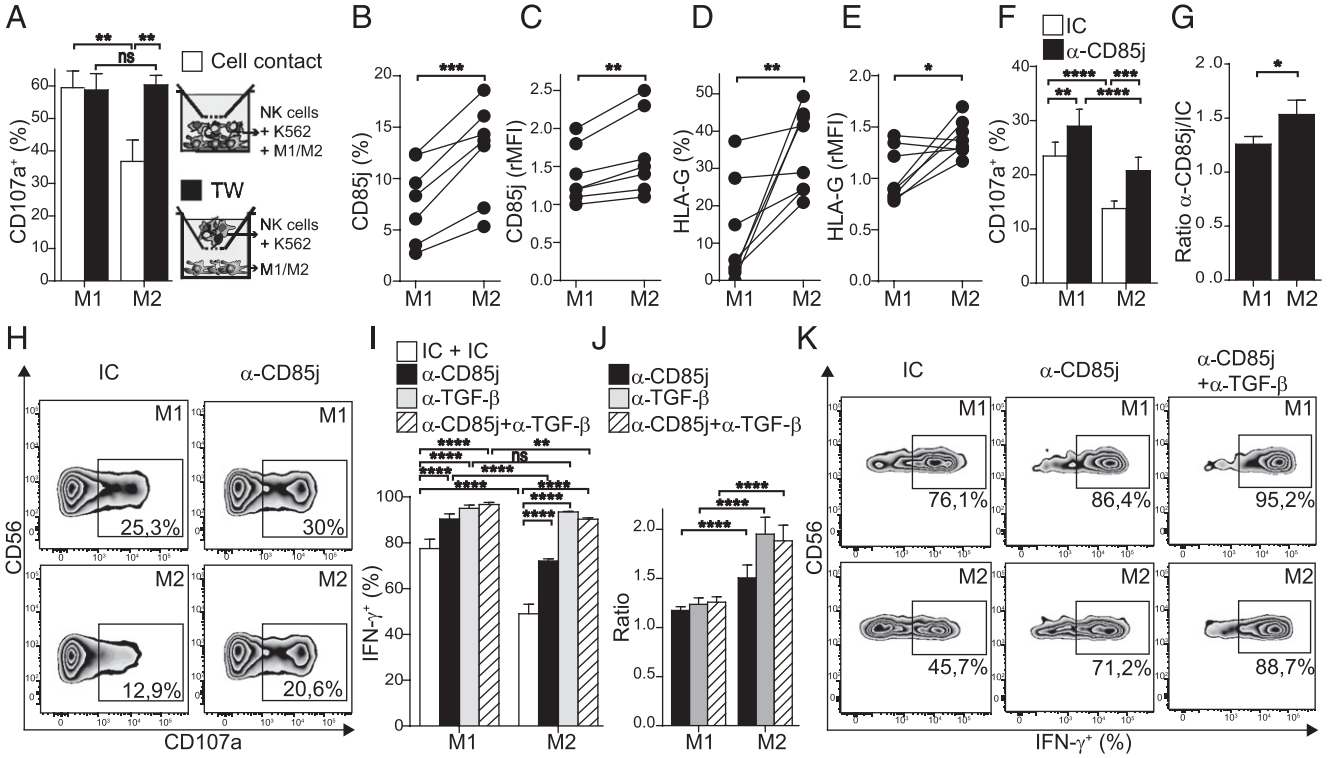

FIGURE 6. Engagement of the inhibitory receptor CD85j (ILT-2) on NK cells exposed to M2 accounts for a reduced NK cell degranulation against susceptible target cells and IFN-γ production. (**A**) Percentage of $CD107a^+CD56^{dim}$ NK cells after coculture with K562 target cells and allogeneic M1 or M2 in the presence of cell-to-cell contact (white bars) or when NK cells and macrophages were separated by transwell devices (TW, black bars). The experimental design is depicted on the right ($n = 4$). (**B** and **C**) Percentage of $CD85j^+$ NK cells (B) or rMFI of CD85j (C) in NK cells after coculture with M1 or M2 ($n = 7$). (**D** and **E**) Percentage (D) or rMFI (E) of HLA-G^+ M1 and M2 cells ($n = 8$). (**F**) Percentage of $CD107a^+CD56^{dim}$ NK cells after coculture with K562 target cells and allogeneic M1 or M2 in the presence of an IC mAb (white bars) or an anti-CD85j blocking mAb (black bars) ($n = 10$). (**G**) Ratio of the percentage of $CD107a^+CD56^{dim}$ NK cells in the presence of an anti-CD85j blocking mAb and the percentage of $CD107a^+CD56^{dim}$ NK cells in the presence of an IC mAb for NK cells cocultured with M1 or M2 ($n = 10$). (**H**) Representative zebra plots from cells from one healthy donor. (**I**) Percentage of IFN-γ^+ $CD56^{bright}$ NK cells after stimulation with IL-12, IL-15, and IL-18, and allogeneic M1 or M2 in the presence of IC mAb (white bars), an anti-CD85j blocking mAb (black bars), an anti–TGF-β blocking mAb (gray bars), or both (cross-hatched bars) ($n = 4$). (**J**) Ratio of the percentage of IFN-γ^+CD56^{bright} NK cells in the presence of the blocking mAb and the percentage of IFN-γ^+CD56^{bright} NK cells in the presence of the IC mAb for NK cells cocultured with M1 or M2 ($n = 4$). (**K**) Representative zebra plots from cells from one healthy donor. A two-way ANOVA with repeated measures matched by both factors and Bonferroni post hoc test was used in (A), (F), (I), and (J). A paired *t* test was used in (B)–(E) and (G). Mean ± SEM were plotted in (A), (F), (G), (I), and (J). Individual values for each donor were plotted in (B)–(E). $^*p < 0.05$, $^{**}p < 0.01$, $^{***}p < 0.001$, $^{****}p < 0.0001$.

mouse IgG2a mAb (the anti-CD85j) to human Fc receptors (Supplemental Fig. 4B).

We also assessed the effect of CD85j blockade on IFN-γ production by $CD56^{bright}$ NK cells blocking or not blocking TGF-β (Fig. 6I–K). Although blockade of TGF-β abundantly restored the percentage of IFN-γ–producing $CD56^{bright}$ NK cells, blockade of CD85j also resulted in a robust restoration (Fig. 6I). Accordingly, blockade of CD85j during coculture of M2 and NK cells led to a significantly higher recovery in the percentage of IFN-γ–producing $CD56^{bright}$ NK cells compared with its blockade during coculture of M1 (Fig. 6J).

Altogether, our results indicate that, in addition to the previously demonstrated role of M2-derived TGF-β, M2 restrain NK cell–mediated cytotoxicity and IFN-γ production through a unique mechanism that involves the upregulation of CD85j on NK cells and the interaction with its cognate ligand HLA-G expressed on M2.

Next, we interrogated whether the suppressive effect triggered by M2 on NK cells depends on a continuous contact between both cells, and if it involves a constant engagement of CD85j. Therefore, after coculture with M1 or M2 for 18 h, NK cells were isolated and further recultured with fresh M1 or M2 or in the absence of macrophages. Also, these NK cells were cultured alone, or were exposed to an IC mAb or an anti-CD85j blocking mAb (Fig. 7A). We observed that the suppressive effect triggered on NK cell degranulation by M2 persisted even in the absence of M2 for at least 2 h and did not depend on a sustained engagement of CD85j, as it lasted even in the presence of an anti-CD85j blocking mAb (Fig. 7B).

Therefore, our results indicate that human M2 limit NK cell effector functions through distinctive mechanisms that involve a TGF-β–mediated suppression of IFN-γ production by $CD56^{bright}$ NK cells, and an upregulation of CD85j that inhibits $CD56^{dim}$ NK cell degranulation and IFN-γ production by $CD56^{bright}$ NK cells triggered by an upregulated expression of HLA-G in M2. Also, these NK cells remained at least transiently hyporesponsive to degranulation stimuli.

Discussion

In this work, we explored the consequences of the interaction of NK cells with anti-inflammatory macrophages using polarized macrophages generated following consensus guidelines (7). M1 secreted higher amounts of IL-12, IL-23, IL-27, and IL-18 than M2. Although mouse M2 secrete higher amounts of IL-10 and TGF-β compared with M1 (7, 9, 10), we observed that human M1 secreted higher amounts of IL-10 and similar amounts of TGF-β compared with M2, similar to the results of others (24–27).

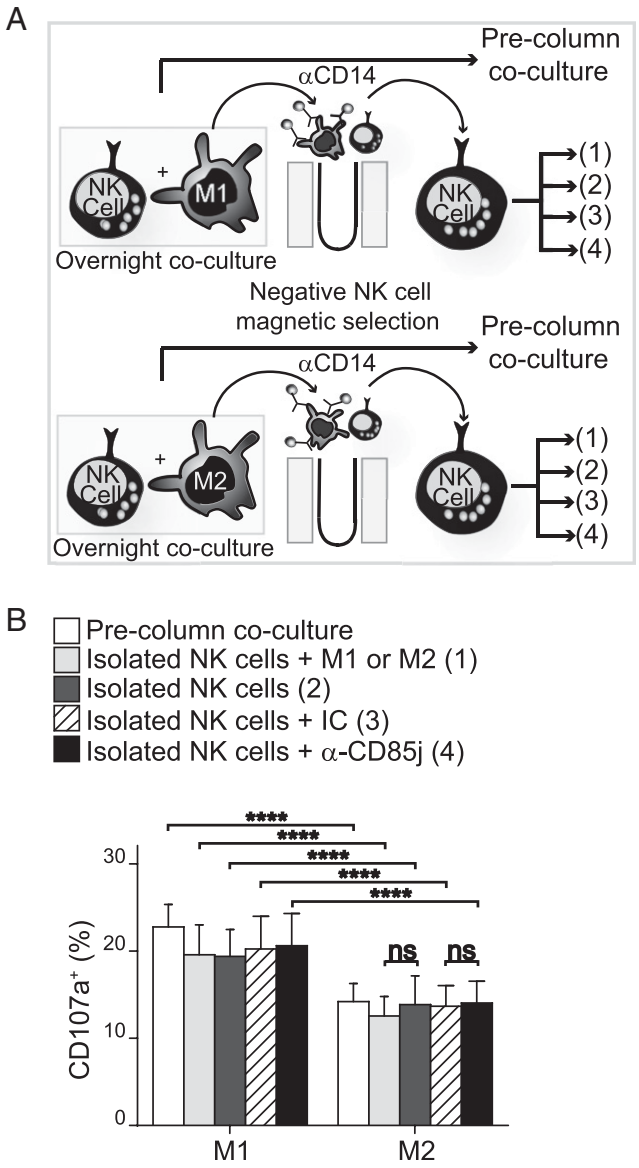

FIGURE 7. Exposure of NK cells to M2 macrophages generates transiently hyporesponsive NK cells. (**A**) Schematic representation of the experimental design used to assess the consequences of the exposure of NK cells to M2. Briefly, NK cells were cocultured with M1 or M2 for 18 h. Thereafter, cells were harvested and NK cells were separated from macrophages by negative immunomagnetic selection of $CD14^+$ cells. Isolated NK cells were further cultured with fresh M1 or M2 (condition 1), in the absence of macrophages (condition 2), in the absence of macrophages but in the presence of an IC mAb (condition 3), or in the absence of macrophages but in the presence of an anti-CD85j blocking mAb (condition 4). Finally, degranulation assays were performed with these NK cells. (**B**) Percentage of $CD107a^+CD56^{dim}$ NK cells after culture of NK cells previously exposed to M1 or M2 as detailed in (A) (conditions 1–4). As control, NK cells that remained in contact with M1 or M2 were also analyzed (precolumn coculture). A two-way ANOVA 1700737with repeated measures matched by both factors and Bonferroni post hoc test was used ($n = 6$). Mean ± SEM were plotted in (B). $****p < 0.0001$.

Nonetheless, the ratio of proinflammatory to anti-inflammatory cytokines was much higher for M1 than for M2, suggesting that they resemble tissue-resident pro- and anti-inflammatory macrophages (28). Moreover, the M2-like phenotype has been associated with tumor progression and reduced overall survival in cancer patients (29).

The consequences of the cross-talk between macrophages and NK cells has been reviewed (13). Human macrophages promote NK cell activation and IFN-γ secretion through a mechanism that involves CD244 (2B4), and cytotoxicity against LPS-treated macrophages in an NKG2D-dependent manner (14). Moreover, the interaction between NKp80 and activation-induced C-type lectin promotes cytokine production and degranulation of NK cells upon cross-talk with M0 (30). M0 and M2 repolarized toward M1 can trigger NK cell activation and effector functions (15), whereas TAMs from ascites from ovarian cancer patients display a M2-skewed phenotype that can be reprogrammed into M1-like macrophages with LPS and subsequently promote IFN-γ production and cytotoxicity by NK cells (12). However, the effects of M2 on NK cells were not explored. We observed that M2 limit NK cell activation (negatively affecting CD25, CD69, and CD56 expression), and IFN-γ production by cytokine-stimulated $CD56^{bright}$ NK cells, which was associated with reduced expression of T-bet, a critical transcription factor that stimulates IFN-γ gene transcription (23). The effect of M2 on IFN-γ production was mediated by soluble TGF-β. TGF-β also restrained IFN-γ production by M1 in $CD56^{bright}$ NK cells, which may constitute a self-control mechanism of proinflammatory macrophages to prevent overactivation of NK cells in inflamed tissues and/or secondary lymphoid organs. Strikingly, our results suggest that M2 overexploit the production of soluble TGF-β to suppress NK cell IFN-γ production. Accordingly, human regulatory T cells inhibit IFN-γ production by NK cells through membrane-bound TGF-β (31).

The suppressive effect of M2 also extends to $CD56^{dim}$ NK cells as they displayed less degranulation and cytotoxicity, associated with a reduction in the content of pfp and granzyme B. This effect required cell-to-cell contact but did not involve membrane-bound TGF-β as was observed for regulatory T cells (31). Instead, M2 induced upregulation of the inhibitory receptor CD85j on NK cells. Similar phenotypic alterations have been observed in blood NK cells from patients with colorectal cancer (32). Blocking experiments demonstrated that NK cells exposed to M2 experienced a higher degree of CD85j engagement as a consequence of both, the upregulated expression of CD85j on NK cells, and a higher expression of HLA-G on M2. This interaction contributed to the generation of $CD56^{dim}$ NK cells with diminished degranulation ability and $CD56^{bright}$ NK cells with lower IFN-γ producing capacity, compared with NK cells exposed to M1. The effect was mediated by CD85j expressed by NK cells and not on macrophages as the recovery in NK cell degranulation upon CD85j blockade was not detected when this receptor was blocked exclusively on M1 or M2. Also, the involvement of CD85j in the inhibition of NK cell effector functions was independent of possible Fc-mediated effects triggered by this mAb because the affinity of mouse IgG2a (the isotype of the anti-CD85j mAb) for human Fc receptors is 250 times lower than the affinity of human IgG (33) and similar results were obtained in the absence or in the presence of an excess of human IgG (the natural ligands for Fc receptors).

Upregulation of an inhibitory receptor such as CD85j in NK cells without affecting the expression of major activating and other inhibitory receptors indicates that M2 may raise the activation threshold of NK cells. Such strategy may constitute an efficient manner to suppress NK cell effector functions because a hypothetical downregulation of an activating receptor may desensitize NK cells only to target cells that express the cognate ligand. Instead, upregulation of an inhibitory receptor such as CD85j would affect the activation threshold of NK cells regardless of the activation receptor used to sense target cells. Accordingly, upregulated expression of CD85j in peripheral blood NK cells from triple-negative breast cancer patients dampens cetuximab-mediated Ab-dependent cellular

cytotoxicity and this effect can be reversed by CD85j blockade (34). Thus, M2 may generate hyporesponsive NK cells with impaired immunosurveillance capacity.

The inhibition of NK cell–mediated cytotoxicity lasted at least for several hours, confirming that M2 generate transiently hyporesponsive NK cells. This effect is probably triggered by interaction between CD85j on $CD56^{dim}$ NK cells and its cognate ligand HLA-G expressed by M2 (35). This circuit might be relevant in the tumor microenvironment where M2-like macrophages may generate hyporesponsive NK cells that subsequently display impaired cytotoxic activity against the tumor cells even without contacting M2-like macrophages. Accordingly, human mammary tumors contain macrophages that express HLA-G and lymphoid cells that express increased amounts of CD85j (36). Thus, expansion of M2-like macrophages may constitute a tumor-driven shield against NK cell effector functions, reinforcing the notion that therapeutic reprogramming of M2-like macrophages constitutes an exciting approach to improve the efficacy of tumor-targeted immunotherapy strategies.

Overall, our results indicate that M2 curb NK cell activation and effector functions through distinctive mechanisms that involve a TGF-β–mediated suppression of IFN-γ production by $CD56^{bright}$ NK cells, and an upregulation of CD85j that inhibits $CD56^{dim}$ NK cell degranulation and IFN-γ production by $CD56^{bright}$ NK cells triggered by an upregulated expression of HLA-G in M2. Moreover, such cross-talk generates transient hyporesponsive NK cells with impaired cytotoxic capacity. Therefore, our results may have implications in different situations where M2-like cells become accumulated such as the resolution of inflammation and tumor environments.

Acknowledgments

We thank Dr. Nora Etchenique and Dr. Marisa Martino from the Instituto de Hemoterapia of the Province of Buenos Aires, Jimena Bernchartе and Dr. Oscar Torres from the Transfusion Medicine of the Hospital Churruca-Visca, Buenos Aires, for providing buffy coats, and Dr. Gabriel A. Rabinovich from the Laboratory of Immunopathology of Instituto de Biología y Medicina Experimental for continued support.

Disclosures

The authors have no financial conflicts of interests.

References

1. Newman, K. C., and E. M. Riley. 2007. Whatever turns you on: accessory-cell-dependent activation of NK cells by pathogens. *Nat. Rev. Immunol.* 7: 279–291.
2. Lanier, L. L. 2008. Up on the tightrope: natural killer cell activation and inhibition. *Nat. Immunol.* 9: 495–502.
3. Carrega, P., and G. Ferlazzo. 2012. Natural killer cell distribution and trafficking in human tissues. *Front. Immunol.* 3: 347.
4. Caligiuri, M. A. 2008. Human natural killer cells. *Blood* 112: 461–469.
5. Strowig, T., F. Brilot, and C. Münz. 2008. Noncytotoxic functions of NK cells: direct pathogen restriction and assistance to adaptive immunity. *J. Immunol.* 180: 7785–7791.
6. Moretta, A., E. Marcenaro, S. Parolini, G. Ferlazzo, and L. Moretta. 2008. NK cells at the interface between innate and adaptive immunity. *Cell Death Differ.* 15: 226–233.
7. Murray, P. J., J. E. Allen, S. K. Biswas, E. A. Fisher, D. W. Gilroy, S. Goerdt, S. Gordon, J. A. Hamilton, L. B. Ivashkiv, T. Lawrence, et al. 2014. Macrophage activation and polarization: nomenclature and experimental guidelines. *Immunity* 41: 14–20.
8. Mosser, D. M., and J. P. Edwards. 2008. Exploring the full spectrum of macrophage activation. *Nat. Rev. Immunol.* 8: 958–969.
9. Porta, C., E. Riboldi, A. Ippolito, and A. Sica. 2015. Molecular and epigenetic basis of macrophage polarized activation. *Semin. Immunol.* 27: 237–248.
10. Martinez, F. O., and S. Gordon. 2014. The M1 and M2 paradigm of macrophage activation: time for reassessment. *F1000Prime Rep.* 6: 13.
11. Sica, A., and A. Mantovani. 2012. Macrophage plasticity and polarization: in vivo veritas. *J. Clin. Invest.* 122: 787–795.
12. Bellora, F., R. Castriconi, A. Dondero, A. Pessino, A. Nencioni, G. Liggieri, L. Moretta, A. Mantovani, A. Moretta, and C. Bottino. 2014. TLR activation of tumor-associated macrophages from ovarian cancer patients triggers cytolytic activity of NK cells. *Eur. J. Immunol.* 44: 1814–1822.
13. Michel, T., F. Hentges, and J. Zimmer. 2013. Consequences of the crosstalk between monocytes/macrophages and natural killer cells. *Front. Immunol.* 3: 403.
14. Nedvetzki, S., S. Sowinski, R. A. Eagle, J. Harris, F. Vély, D. Pende, J. Trowsdale, E. Vivier, S. Gordon, and D. M. Davis. 2007. Reciprocal regulation of human natural killer cells and macrophages associated with distinct immune synapses. *Blood* 109: 3776–3785.
15. Bellora, F., R. Castriconi, A. Dondero, G. Reggiardo, L. Moretta, A. Mantovani, A. Moretta, and C. Bottino. 2010. The interaction of human natural killer cells with either unpolarized or polarized macrophages results in different functional outcomes. *Proc. Natl. Acad. Sci. USA* 107: 21659–21664.
16. Komohara, Y., H. Hasita, K. Ohnishi, Y. Fujiwara, S. Suzu, M. Eto, and M. Takeya. 2011. Macrophage infiltration and its prognostic relevance in clear cell renal cell carcinoma. *Cancer Sci.* 102: 1424–1431.
17. Leek, R. D., C. E. Lewis, R. Whitehouse, M. Greenall, J. Clarke, and A. L. Harris. 1996. Association of macrophage infiltration with angiogenesis and prognosis in invasive breast carcinoma. *Cancer Res.* 56: 4625–4629.
18. Nishie, A., M. Ono, T. Shono, J. Fukushi, M. Otsubo, H. Onoue, Y. Ito, T. Inamura, K. Ikezaki, M. Fukui, et al. 1999. Macrophage infiltration and heme oxygenase-1 expression correlate with angiogenesis in human gliomas. *Clin. Cancer Res.* 5: 1107–1113.
19. Allavena, P., A. Sica, C. Garlanda, and A. Mantovani. 2008. The Yin-Yang of tumor-associated macrophages in neoplastic progression and immune surveillance. *Immunol. Rev.* 222: 155–161.
20. Wu, Y., D. M. Kuang, W. D. Pan, Y. L. Wan, X. M. Lao, D. Wang, X. F. Li, and L. Zheng. 2013. Monocyte/macrophage-elicited natural killer cell dysfunction in hepatocellular carcinoma is mediated by CD48/2B4 interactions. *Hepatology* 57: 1107–1116.
21. Gillard-Bocquet, M., C. Caer, N. Cagnard, L. Crozet, M. Perez, W. H. Fridman, C. Sautès-Fridman, and I. Cremer. 2013. Lung tumor microenvironment induces specific gene expression signature in intratumoral NK cells. *Front. Immunol.* 4: 19.
22. Rossi, L. E., D. E. Avila, R. G. Spallanzani, A. Ziblat, M. B. Fuertes, L. Lapyckyj, D. O. Croci, G. A. Rabinovich, C. I. Domaica, and N. W. Zwirner. 2012. Histone deacetylase inhibitors impair NK cell viability and effector functions through inhibition of activation and receptor expression. *J. Leukoc. Biol.* 91: 321–331.
23. Ziblat, A., C. I. Domaica, R. G. Spallanzani, X. L. Iraolagoitia, L. E. Rossi, D. E. Avila, N. I. Torres, M. B. Fuertes, and N. W. Zwirner. 2015. IL-27 stimulates human NK-cell effector functions and primes NK cells for IL-18 responsiveness. *Eur. J. Immunol.* 45: 192–202.
24. Raggi, F., S. Pelassa, D. Pierobon, F. Penco, M. Gattorno, F. Novelli, A. Eva, L. Varesio, M. Giovarelli, and M. C. Bosco. 2017. Regulation of human macrophage M1-M2 polarization balance by hypoxia and the triggering receptor expressed on myeloid cells-1. *Front. Immunol.* 8: 1097.
25. Mia, S., A. Warnecke, X. M. Zhang, V. Malmström, and R. A. Harris. 2014. An optimized protocol for human M2 macrophages using M-CSF and IL-4/IL-10/TGF-β yields a dominant immunosuppressive phenotype. *Scand. J. Immunol.* 79: 305–314.
26. Vogel, D. Y., J. E. Glim, A. W. Stavenuiter, M. Breur, P. Heijnen, S. Amor, C. D. Dijkstra, and R. H. Beelen. 2014. Human macrophage polarization in vitro: maturation and activation methods compared. *Immunobiology* 219: 695–703.
27. Tarique, A. A., J. Logan, E. Thomas, P. G. Holt, P. D. Sly, and E. Fantino. 2015. Phenotypic, functional, and plasticity features of classical and alternatively activated human macrophages. *Am. J. Respir. Cell Mol. Biol.* 53: 676–688.
28. Gordon, S., A. Plüddemann, and F. Martinez Estrada. 2014. Macrophage heterogeneity in tissues: phenotypic diversity and functions. *Immunol. Rev.* 262: 36–55.
29. Elliott, L. A., G. A. Doherty, K. Sheahan, and E. J. Ryan. 2017. Human tumor-infiltrating myeloid cells: phenotypic and functional diversity. *Front. Immunol.* 8: 86.
30. Welte, S., S. Kuttruff, I. Waldhauer, and A. Steinle. 2006. Mutual activation of natural killer cells and monocytes mediated by NKp80-AICL interaction. *Nat. Immunol.* 7: 1334–1342.
31. Ghiringhelli, F., C. Ménard, M. Terme, C. Flament, J. Taieb, N. Chaput, P. E. Puig, S. Novault, B. Escudier, E. Vivier, et al. 2005. CD4+CD25+ regulatory T cells inhibit natural killer cell functions in a transforming growth factor-beta-dependent manner. *J. Exp. Med.* 202: 1075–1085.
32. Rocca, Y. S., M. P. Roberti, E. P. Juliá, M. B. Pampena, L. Bruno, S. Rivero, E. Huertas, F. Sánchez Loria, A. Pairola, A. Caignard, et al. 2016. Phenotypic and functional dysregulated blood NK cells in colorectal cancer patients can be activated by cetuximab plus IL-2 or IL-15. *Front. Immunol.* 7: 413.
33. Lubeck, M. D., Z. Steplewski, F. Baglia, M. H. Klein, K. J. Dorrington, and H. Koprowski. 1985. The interaction of murine IgG subclass proteins with human monocyte Fc receptors. *J. Immunol.* 135: 1299–1304.
34. Roberti, M. P., E. P. Juliá, Y. S. Rocca, M. Amat, A. I. Bravo, J. Loza, F. Coló, C. M. Loza, V. Fabiano, M. Maino, et al. 2015. Overexpression of CD85j in TNBC patients inhibits Cetuximab-mediated NK-cell ADCC but can be restored with CD85j functional blockade. *Eur. J. Immunol.* 45: 1560–1569.
35. Takahashi, H., K. Sakakura, T. Kudo, M. Toyoda, K. Kaira, T. Oyama, and K. Chikamatsu. 2017. Cancer-associated fibroblasts promote an immunosuppressive microenvironment through the induction and accumulation of protumoral macrophages. *Oncotarget* 8: 8633–8647.
36. Lefebvre, S., M. Antoine, S. Uzan, M. McMaster, J. Dausset, E. D. Carosella, and P. Paul. 2002. Specific activation of the non-classical class I histocompatibility HLA-G antigen and expression of the ILT2 inhibitory receptor in human breast cancer. *J. Pathol.* 196: 266–274.